Solar chimney power plant performance characteristics

D.G. Kröger[1] J.D. Buys[2]

(First received November 2001; Final version May 2002)

The performance characteristics of a large solar chimney power plant are evaluated. The reference plant studied has a glass-covered collector and a chimney that is 1 500 m high with a diameter of 160 m. A turbo-generator is located at the base of the chimney. The draught and relevant energy equations applicable to the plant are solved for specified meteorological data at a particular site in South Africa. It is shown that the output of the plant changes measurably during the day and that power is also generated during the night, due to the thermal capacity of the ground under the solar collector. By optimising the shape and height of the solar collector, the annual power output can be increased.

Nomenclature

b	exponent
C_D	drag coefficient
C_E	extinction coefficient
c_p	specific heat, J/kg K
d	diameter, m
e	surface roughness
f	friction factor
H	height, m
h	heat transfer coefficient, W/m^{2}K
I	solar radiation, W/m^2
K	loss coefficient
k	thermal conductivity, W/mK
m	mass flow rate, kg/s
n	number
P	pitch, m or power, W
p	pressure, N/m^2
Pr	Prandtl
q	heat transfer rate, W/m^2
R	gas constant, J/kg K
Re	Reynolds number
r	radius, m
T	temperature, K or °C
t	thickness, m or time, s
v	velocity, m/s
z	co-ordinate or depth, m

Greek

α	absorptance
Δ	differential
ε	emissivity
η	efficiency
σ	Boltzmann constant, W/m^{2}K^4
ρ	density, kg/m^3 or reflectance
θ	angle
τ	transmissivity

Subscripts

a	ambient or air or absorptance
b	beam
acc	acceleration
c	chimney
i	inlet
o	outlet
p	pressure
r	radial or roof or radiation
D	drag or Darcy
d	diffuse
f	friction
g	ground
h	convective heat transfer
s	support or sky
sky	sky
t	turbine or transversal
tg	turbo-generator
w	wind

Introduction

A solar chimney power plant consists of a central chimney, surrounded by a solar collector that consists of a transparent canopy or roof supported a few metres above ground level, as shown in Fig. 1.

A turbine driving a generator is located at the base of the chimney. Solar radiation passing through the canopy strikes the ground below it from where heat is transferred to the adjacent air by means of convection. Due to buoyancy, the heated air flows towards the centre of the collector and then up the chimney where it drives the turbine.

Tests conducted at an experimental solar chimney power plant located at Manzanares in Spain have shown that the concept is sound and that performance trends are in line with predicted values.[1,2] Preliminary studies have indicated that large solar chimney power plants are potentially economically viable.[3,4]

In this study, the performance characteristics of a large

1. Department of Mechanical Engineering, University of Stellenbosch, Private Bag X1, Matieland, 7602 South Africa (dgk@maties.sun.ac.za)

2. Department of Mechanical Engineering, University of Stellenbosch

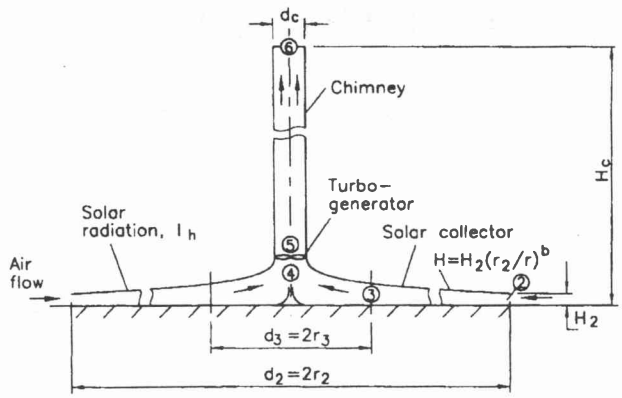

Fig. 1. Solar chimney power plant

solar chimney reference power plant, having dimensions as listed in Appendix A, were determined for meteorological conditions as given in Tables A1 and A2. These latter conditions are applicable at a site located near Sishen (27.67° South, 23.00° East) in South Africa. It was shown that the performance of the reference plant can be improved by modifying the collector geometry.

Analysis

To find the power generated by a solar chimney power plant, as shown schematically in Fig. 1, the relevant draught and energy equations have to be solved simultaneously.

1. The power output of the plant can be expressed as

$$\begin{aligned} P = \; & \eta_{tg}\,(\text{driving potential} - \textstyle\sum \text{pressure drop}) \\ & \times \text{air volume flow rate through turbine} \\ = \; & \eta_{tg}\left[\begin{array}{l}\Delta p - \\ \left(\begin{array}{l}\Delta p_i + \Delta p_s + \Delta p_{acc} \\ +\Delta p_f + \Delta p_{ti} + \Delta p_{cD} \\ +\Delta p_{cacc} + \Delta p_{cf} + 0.5\rho_6 v_6{}^2\end{array}\right)\end{array}\right] m/\rho_{ti} \end{aligned} \tag{1}$$

where η_{tg} is the efficiency of the turbo-generator.

The pressure difference due to a column of cold air outside the chimney and a column of hot air inside the chimney is the driving force or potential that causes the air to flow through the plant. Blaine & Kröger[5] evaluate the effect of different ambient conditions on the potential and show that for the case where adiabatic lapse rates are assumed outside and inside the chimney

$$\Delta p = \; p_1\left[1 - \left\{\begin{array}{c}(1 - 0.00975H_c/T_1)\,/ \\ (1 - 0.00975H_c/T_3)\end{array}\right\}^{3.5}\right] \tag{2}$$

The pressure drop between the essentially stagnant ambient air at 1 and at the inlet 2 to the collector is given by

$$\Delta p_i = (p_1 - p_2) = K_i\rho_2 v_2^2/2 + \rho_2 v_2^2/2 \tag{3}$$

where K_i is the collector inlet loss coefficient.

Canopy supports are arranged radially with a radial pitch P_r and a tangential pitch P_t. Air flowing radially inwards in the solar collector experiences a pressure drop across a circle of supports at a particular radius. If the height of the canopy or roof is given by $H = H_2(r_2/r)^b$ this pressure drop is

$$dp_s = C_{sD}m^2 d_s r^{2(b-1)}/\left(8\pi^2\rho P_t H_2^2 r_2^{2b}\right) \tag{4}$$

where C_{sD} is the drag coefficient of the particular support and m is the radial air mass flow rate.[6]

The pressure drop due to all supports is obtained by the following summation:

$$\Delta p_s = \frac{C_{sD}m^2 d_s}{8\pi^2 P_t H_2^2 r_2^{2b}} \sum_{n_s=0}^{n_s=n_{st}} \frac{(r_2 - n_s P_r)^{2(b-1)}}{\rho_{ns}} \tag{5}$$

where n_{st} is the total number of support circles.

As the air flows radially inwards it accelerates (if $b < 1$) with the result that the pressure drops:[6]

$$\Delta p_{acc} = \int_{r_2}^{r_3} dp = -\int_{r_2}^{r_3}\left[m^2 R r^{(b-1)}/\left(4\pi^2 p H_2^2 r_2^2\right)\right]\partial\left(T/r^{(b-1)}\right) \tag{6}$$

The pressure drop Δp_f due to frictional effects under the collector are given by Kröger & Buys[7] and Beyers[8] while the pressure drop across the turbine inlet Δp_{ti} can be expressed in terms of a specified turbine inlet loss coefficient K_{ti}. Similarly, the pressure drop Δp_{cD} due to the drag of appurtenances such as spokes or other reinforcements inside the chimney can be expressed in terms of a loss coefficient K_{cD}.

For a chimney of constant cross-sectional area, the change in pressure due to the change in momentum, be-

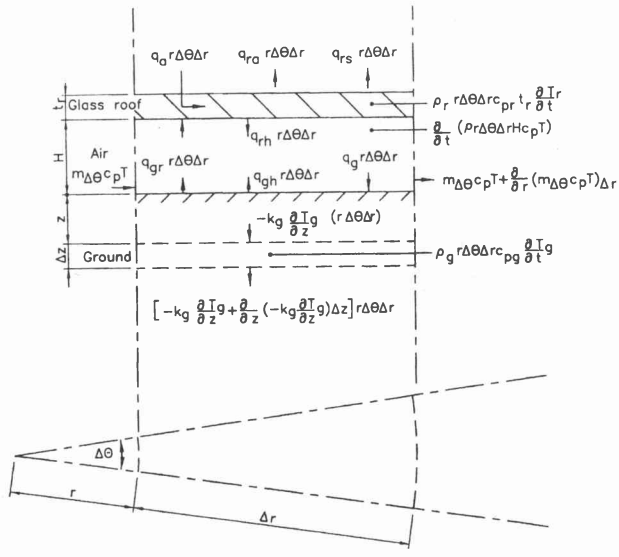

Fig. 2. Control volumes in collector

tween the inlet and the outlet of the chimney, can be expressed as

$$\Delta p_{cacc} = \left[4m/\left(\pi d_c^2\right)\right]^2 \left(1/\rho_6 - 1/\rho_4\right) \tag{7}$$

If it is assumed that the turbulent flow in the chimney is fully developed, the frictional loss can be expressed approximately as

$$\Delta p_{cf} = f_c \left(H_6 - H_5\right) \left[4m/\left(\pi d_c^2\right)\right]^2 / \left(2\rho_4 d_c\right) \tag{8}$$

where according to Haaland[9]

$$f_c = 2.7778 \left[\log_{10}\left\{\left(\frac{7.7}{\mathrm{Re}_c}\right)^3 + \left(\frac{e_c}{3.75 d_c}\right)^{3.33}\right\}\right]^{-2} \tag{9}$$

where e_c is the surface roughness of the concrete.

2. The energy equation applicable to the elementary control volume about the air stream in the collecter as shown in Fig. 2 is

$$\begin{aligned} &\frac{\partial}{\partial r}\left(m_{\Delta\theta} c_p T\right) \Delta r + \frac{\partial}{\partial t}\left(\rho\ r\ \Delta\ \theta\ \Delta r\ H\ c_p\ T\right) \\ &= q_{gh} r \Delta\theta \Delta r + q_{rh}\ r\ \Delta\ \theta\ \Delta r \end{aligned} \tag{10}$$

Since $\rho = p/RT$ and changes in c_p and p are negligible, this equation together with the continuity relation $\partial/\partial r\left(m_{\Delta\theta}\right)\Delta r = -\partial/\partial t\left(\rho\ r\ \Delta\ \theta\ \Delta r\ H\right)$ can be simplified to give for fully developed flow

$$\begin{aligned} &\rho\ c_p\ H \frac{\partial T}{\partial t} + \left(\frac{m c_p}{2\pi r}\right)\frac{\partial T}{\partial r} = q_{gh} + q_{rh} \\ &= h_g\left(T_g - T\right) + h_r\left(T_r - T\right) \end{aligned} \tag{11}$$

According to Gnielinski,[10] the heat transfer coefficients under the roof and on the ground for fully developed flow can be expressed as

$$\begin{aligned} &h = k\left(f_D/16\right)\left(\mathrm{Re} - 1\ 000\right)\mathrm{Pr}\ / \\ &\left[H\left\{1.07 + 12.7\left(f_D/8\right)^{0.5}\left(\mathrm{Pr}^{0.67} - 1\right)\right\}\right] \end{aligned} \tag{12}$$

For developing flow near the inlet of the collector

$$\begin{aligned} &\rho\ c_p\ H \frac{\partial T}{\partial t} + \left(\frac{m c_p}{2\pi r}\right)\frac{\partial T}{\partial r} = q_{gh} + q_{rh} \\ &= h_g\left(T_g - T_a\right) + h_r\left(T_r - T_a\right) \end{aligned} \tag{13}$$

Kröger & Buys[7] give values for h for developing flow under the roof and on the ground.

3. Assume that the temperature difference between the top and bottom surfaces of the glass roof is negligible and apply an energy balance to the elementary control volume shown in Fig. 2:

$$q_a + q_{gr} - q_{rh} - q_{ra} - q_{rs} = \rho_r c_{pr} t_r \partial T_r/\partial t \tag{14}$$

where q_a is the heat absorbed by the glass, i.e.

$$q_a = \frac{\left(1 - \rho_b\right)\left(1 - \tau_{ba}\right) I_b}{\left(1 - \rho_b \tau_{ba}\right)} + \frac{\left(1 - \rho_d\right)\left(1 - \tau_{da}\right) I_d}{\left(1 - \rho_d \tau_{da}\right)} \tag{15}$$

where the total radiation per unit area of horizontal surface is

$$I_h = I_b + I_d. \tag{16}$$

According to Duffie & Beckman[11] the beam reflectance at the upper surface of the glass can be expressed as

$$\rho_b = \frac{1}{2}\left[\begin{array}{l} \dfrac{\sin^2\left\{\arcsin\left(\sin\theta/1.526\right) - \theta\right\}}{\sin^2\left\{\arcsin\left(\sin\theta/1.526\right) + \theta\right\}} \\ \\ + \dfrac{\tan^2\left\{\arcsin\left(\sin\theta/1.526\right) - \theta\right\}}{\tan^2\left\{\arcsin\left(\sin\theta/1.526\right) + \theta\right\}} \end{array}\right] \tag{17}$$

where θ is the zenith angle of incidence. For diffuse radiation the approximate reflectance is determined at $\theta = 60°$ i.e. $\rho_d = 0.0934$.

The beam transmittance through the glass roof due to absorption is given by

$$\tau_{ba} = e^{-C_e t_r/\left[\cos\left\{\arcsin\left(\sin\theta/1.526\right)\right\}\right]}. \tag{18}$$

The transmittance of diffuse radiation considering only absorption, τ_{da} is the same as that of τ_{ba} evaluated at $\theta = 60°$.

The net longwave radiation heat transfer rate betwseen the ground and the roof is given by

$$q_{gr} = \sigma\left(T_g{}^4 - T_r{}^4\right) / \left(1/\varepsilon_g + 1/\varepsilon_r - 1\right). \tag{19}$$

The convective heat transfer rate from the glass roof to the air stream under the roof for fully developed flow is given by

$$q_{rh} = h_r\left(T_r - T\right) \tag{20}$$

and

$$q_{rh} = h_r\left(T_r - T_a\right) \tag{21}$$

for developing flow at the inlet of the collector.

The convective heat transfer rate from the roof to the ambient air is given by

$$q_{ra} = h_{ra}\left(T_r - T_a\right)\ . \tag{22}$$

Presently, no reliable equation exists for the convective heat transfer coefficient h_{ra}. The following relation will be employed:[11]

$$h_{ra} \approx 5.7 + 3.8 v_w \tag{23}$$

where v_w is the wind speed at the roof elevation.

The net longwave radiation heat transfer rate between the glass roof and the clear sky is expressed as

$$q_{rs} = \varepsilon_r \sigma\left(T_r{}^4 - T_{sky}^4\right) \tag{24}$$

where the sky temperature according to Swinbank[12] is given by

$$T_{sky} = 0.0552 T_a^{1.5} \tag{25}$$

4. The energy equation applicable to the elementary control volume in the ground (assuming thermophysical properties of ground are constant) as shown in Fig. 2 is given by

$$\rho_g c_{pg} \frac{\partial T_g}{\partial t} = k_g \frac{\partial^2 T_g}{\partial z^2} \ . \tag{26}$$

To solve this equation the following conditions are applicable: At $z = 0$

$$k_g \frac{\partial T_g}{\partial z} = q_{gh} + q_{gr} - q_g \ . \tag{27}$$

The net solar radiation per unit area absorbed by the ground is[13]

$$\begin{aligned} q_g \ = \ & \frac{(1-\rho_b)^2 \tau_{ba} \alpha_g \ I_b}{(1-\rho_b^2 \tau_{ba}^2)\left[1-\rho_d (1-\alpha_g)\right]} \\ & + \frac{(1-\rho_d)^2 \tau_{da} \alpha_g \ I_d}{(1-\rho_d^2 \tau_{da}^2)\left[1-\rho_d (1-\alpha_g)\right]} \end{aligned} \tag{28}$$

At $z = \infty$, $\partial T_g / \partial z = 0$.

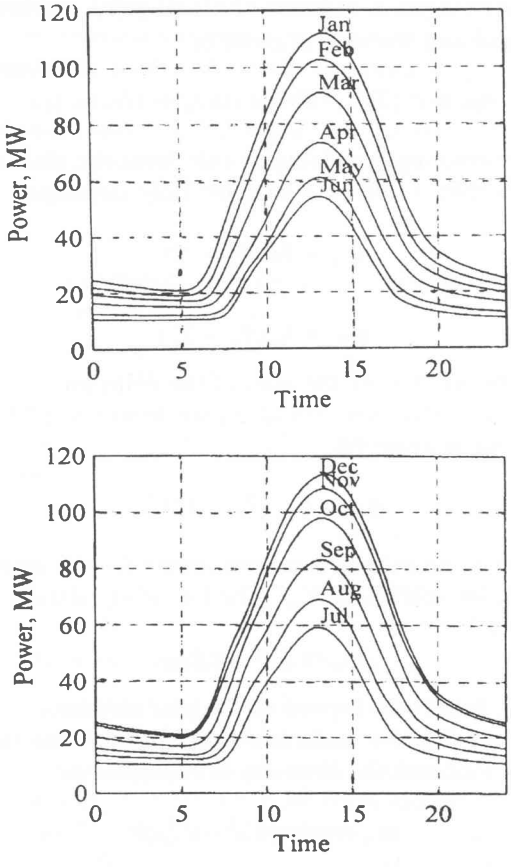

Fig. 3. Maximum electrical output of reference plant

Numerical simulation

The performance of the solar chimney power plant is determined by maximizing the power output:

$$\frac{\partial P}{\partial m} + \frac{\partial P}{\partial T_3} \frac{\partial T_3}{\partial m} = 0 \tag{29}$$

Equations (11), (14), (26), and (27) are semi-discretized by replacing spatial derivatives with finite difference approximations. The resulting equations together with equation (29) are a set of differential-algebraic equations which can be solved numerically using a standard computer code such as DASSL.[14]

Results

The maximum electrical power output of the reference plant on the 21st of each month is shown in Fig. 3.

There is a pronounced peak output shortly after midday and a significant difference in output during the summer and winter months. Due to the heat stored in the ground some power is also generated at night.

Examples of the temperature distributions in the ground under the collector at a radius of 200 m at different times of the day in December and in June are shown in Fig. 4 and Fig. 5. The former shows conditions near the surface of the ground more clearly.

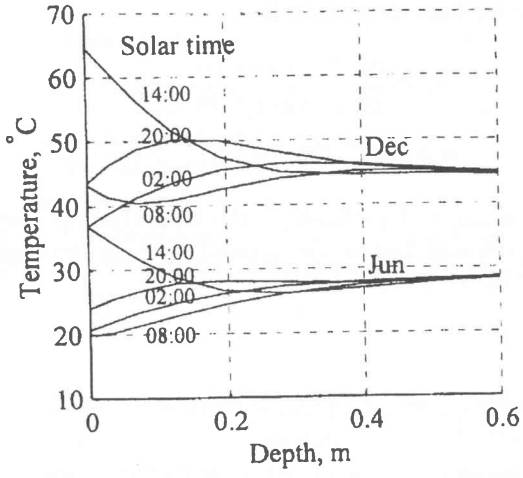

Fig. 4. Temperature distribution in ground near surface

The output of the reference plant, which is 341 GWh/a, can be increased by changing the shape of the collector roof and its inlet height H_2. As shown in Fig. 6 a maximum power output is attained when $b = 1$ and $H_2 = 3.3$ m. For values of $b > 1$ output decreases and there is a danger of flow separation in the collector due to the fact that the flow area increases.

By enlarging the collector area the annual power output can be increased. This is shown graphically in Fig. 7 for $b = 1$. At every collector diameter there is a corresponding optimal inlet height.

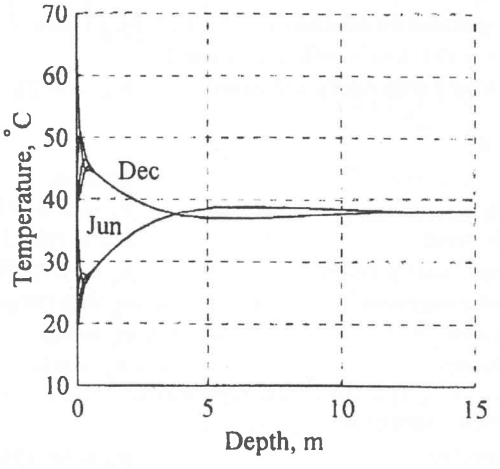

Fig. 5. Temperature distribution in ground

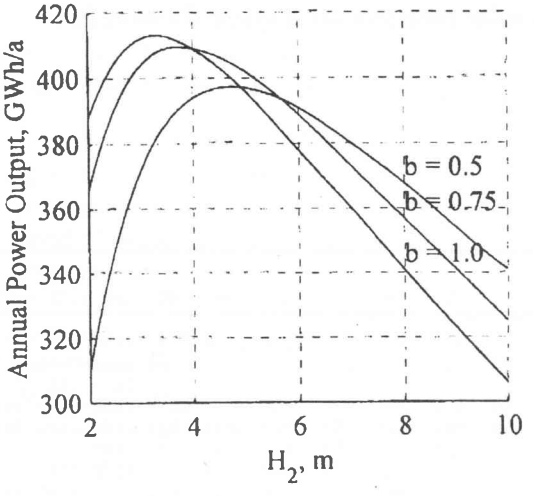

Fig. 6. Annual power output as function of b and H_2

Conclusion

The performance characteristics of a large solar chimney power plant are determined. It is shown that in such a plant there is a pronounced peak output shortly after solar noon, whilst power is also generated at night due to the energy storage capacity of the ground. The output of the reference plant considered can be increased by modifying the shape and inlet height of the solar collector. A further increase in power output can be attained by increasing the collector diameter. Due to greater heating of the air under the collector with increasing collector diameter, heat losses to the environment will also increase. For the particular plant under investigation the nett increase in annual power output is approximately linear over the range of collector diameters shown in Fig. 7.

References

[1] Haaf W, Friedrich KG & Schlaich J. Solar Chimneys. Part 1: Principle and Construction of the Pilot Plant in Manzanares. *Int. J. Solar Energy*, 1983, **2**, pp.3–20.

[2] Haaf W. Solar Chimneys. Part 2: Preliminary Test Results from the Manzanares Plant. *Int. J. Solar Energy*, 1983, **2**, pp.141–161.

[3] Schlaich J & Schiel W. *Solar Chimneys, Encyclopedia of Physical Science and Technology*, 3rd edn, 2000.

[4] Schlaich J. Tension Structures for Solar Electricity Generation. *Engineering Structures*, 1999, **21**, pp.658–668.

[5] Blaine DC & Kröger DG. Analysis of the Driving Potential of a Solar Chimney Power Plant. *R & D Journal*, 1999, **15**, pp.85–94.

[6] Hedderwick RA. Performance Evaluation of a Solar Chimney Power Plant. MSc(Eng) thesis, University of Stellenbosch, Stellenbosch, South Africa, 2001.

[7] Kröger DG & Buys JD. Radial Flow Boundary Layer Development Analysis. *R & D Journal*, 1999, **15**, pp.95–102.

[8] Beyers M. Finite Volume Method for the Analysis of the Thermoflow Field of a Solar Chimney Collector. MSc(Eng) thesis, University of Stellenbosch, South Africa, 2000.

[9] Haaland SE. Simple Explicit Formulas for the Friction Factor in Turbulent Pipe Flow. *Trans. ASME, J. Fluids Engineering*, 1983, **105**, pp.89–90.

[10] Gnielinski V. *Forsch. Ing. Wesen*, 1975, **41**.

[11] Duffie JA & Beckman WA. *Solar Engineering of Thermal Processes*. Wiley Interscience, New York, 1974.

[12] Swinbank WC. Long-wave Radiation from Clear Skies. *Quart. J.R. Meteorol. Soc.*, 1963, **89**.

[13] Modest MF. *Radiative Heat Transfer*. McGraw Hill, New York, 1993.

[14] Brenan KE, Campbell SL & Petzold LR. Numerical Solution of Initial-value Problems in Differential-Algebraic Equations. *SIAM*, 1996.

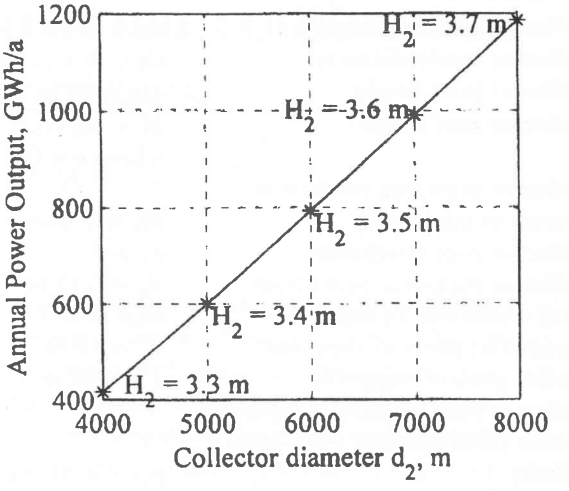

Fig. 7. Annual power output as function of collector diameter ($b = 1$)

Appendix A

For purposes of comparison a reference solar chimney plant and its operating environment is defined.

Power plant specifications:

a. Chimney

Chimney height	$H_c = 1\,500$ m
Chimney inside diameter	$d_c = 160$ m
Chimney drag coefficient due to appurtances (based on chimney cross-sectional area)	$K_{cD} = 0.1$
Chimney inside surface roughness	$e_c = 2 \times 10^{-3}$ m

b. Collector

Collector outside diameter	$d_2 = 2r_2 = 4\ 000$ m
Collector inside diameter	$d_3 = 2r_3 = 400$ m
Collector inlet height	$H_2 = 10$ m
Collector roof shape	$H = H_2 (r_2/r)^b$ where $b = 0.5$
Collector inlet loss coefficient (based on inlet area)	$K_i = 1$
Collector roof roughness	$e_r = 0$
Collector supports (diameter)	$d_s = 0.15$ m
Drag coefficient of supports	$C_{sD} = 1$
Tangential pitch of supports	$P_t = 10$ m
Radial pitch of supports	$P_r = 10$ m
Collector roof material properties: (5 mm thick green of edge glass)	
Density	$\rho_r = 2\ 700$ kg/m^3
Specific heat	$c_{pr} = 840$ J/kg K
Thermal conductivity	$k_r = 0.78$ W/mK
Thickness	$t_r = 0.005$ m
Extinction coefficient	$C_e = 32$/m
Emissivity	$\varepsilon_r = 0.87$
Collector upper convective heat transfer coefficient	$h_a = 5.7$ W/m^2 K

c. Turbine

Turbo-generator efficiency	$\eta_{tg} = 0.8$
Turbine inlet loss coefficient based on turbine cross-sectional area)	$K_{ti} = 0.25$

d. Ground

Type	granite
Density	$\rho_g = 2\ 640$ kg/m^3
Specific heat	$c_{pg} = 820$ J/kg K
Thermal conductivity	$k_g = 1.73$ W/mK
Ground roughness	$e_g = 0.05$ m
Emissivity	$\varepsilon_g = 0.9$
Absorbance	$\alpha_g = 0.9$

e. Ambient conditions

Air pressure	$p_a = 90\ 000$ N/m^2
Wind speed	$v_w = 0$ m/s

Air temperatures are presented in Table A.1, whilst details of the solar radiation are given in Table A.2.

Table A.1 Ambient air temperature

Solar time	1	2	3	4	5	6	7	8	9	10	11	12	13	14	15	16	17	18	19	20	21	22	23	24
Jan	25.52	25.09	24.66	24.33	23.80	23.37	22.94	22.51	24.10	25.9	27.6	29.0	30.0	30.5	30.7	30.5	30.1	29.30	28.10	27.67	27.24	26.81	26.38	25.95
Feb	24.89	24.46	24.03	23.60	23017	22.72	22.31	21.88	22.70	24.5	26.2	27.6	28.7	29.4	29.5	29.3	28.7	27.90	27.47	27.04	26.61	26.18	25.75	25.32
Mar	22.59	22.16	21.73	21.30	20.87	20.44	20.01	19.58	20.70	22.8	24.5	25.9	26.8	27.4	27.5	27.3	26.5	25.60	25.17	24.74	24.31	23.88	23.45	23.02
Apr	18.19	17.76	17.33	16.90	16.47	16.04	15.61	15.18	16.50	18.8	20.6	22.0	23.0	23.6	23.9	23.6	23.0	21.20	20.77	20.34	19.91	19.48	19.05	18.62
May	15.96	15.53	15.10	14.67	14.24	13.81	13.38	12.95	12.52	14.8	16.9	18.4	19.5	20.2	20.4	20.3	19.4	18.97	18.54	18.11	17.68	17.25	16.82	16.39
Jun	13.16	12.73	12.30	11.87	11.44	11.01	10.58	10.15	9.72	11.3	13.6	15.4	16.5	17.3	17.7	17.5	16.6	16.17	15.74	15.31	14.88	14.45	14.02	13.59
Jul	14.06	13.63	13.20	12.77	12.34	11.91	11.48	11.05	10.62	11.4	13.8	15.7	17.0	17.9	18.3	18.2	17.5	17.07	16.64	16.21	15.78	15.35	14.92	14.49
Aug	14.79	14.36	13.93	13.50	13.07	12.64	12.21	11.78	11.35	13.7	15.9	17.7	19.1	20.0	20.5	20.5	19.9	17.80	17.37	16.94	16.51	16.08	15.65	15.22
Sep	19.59	19.16	18.73	18.30	17.87	17.44	17.01	16.58	16.15	18.5	20.6	22.2	23.5	24.3	24.7	24.7	24.1	22.60	22.17	21.74	21.31	20.88	20.45	20.02
Oct	22.09	21.66	21.23	20.80	20.37	19.94	19.51	19.08	19.40	21.5	23.3	24.8	25.9	26.6	26.9	26.9	26.3	25.20	24.67	24.24	23.81	23.38	22.95	22.52
Nov	22.52	22.09	21.66	21.23	20.80	20.37	19.94	20.00	22.20	24.1	25.7	27.0	27.9	28.5	28.6	28.4	27.9	27.00	25.10	24.67	24.24	23.81	23.38	22.95
Dec	24.92	24.49	24.06	23.63	23.20	22.77	22.34	21.91	24.00	25.8	27.4	28.6	29.7	30.1	30.4	30.3	29.7	28.90	27.50	27.07	26.64	26.21	25.78	25.35

Table A.2 Total (I_h) and diffuse (I_d) solar radiation on a horizontal surface, W/m^2

	6		7		8		9		10		11		12		13		14		15		16		17		18	
	I_h	I_d	I_h	I_d	I_h	I_d	I_h	I_d	I_h	I_d	I_h	I_d	I_h	I_d	I_h	I_d	I_h	I_d	I_h	I_d	I_h	I_d	I_h	I_d	I_h	I_d
Jan	138	52	357	89	572	108	762	126	909	136	1003	140	1035	135	1003	140	909	136	762	130	572	114	357	82	138	40
Feb	68	46	279	86	496	109	691	124	845	144	942	151	976	156	942	160	845	161	691	145	496	114	279	75	68	24
Mar	0	0	190	72	406	102	604	121	763	130	865	138	900	144	865	138	763	145	604	133	406	102	180	54	0	0
Apr	0	0	100	50	299	84	489	112	644	129	745	134	780	148	745	142	644	129	489	108	299	78	110	31	0	0
May	0	0	35	18	220	66	407	85	562	101	664	106	700	105	664	100	562	96	407	77	220	48	35	11	0	0
Jun	0	0	19	10	190	63	368	88	517	109	616	117	650	111	616	105	517	93	368	70	190	44	19	6	0	0
Jul	0	0	35	17	220	66	407	90	562	107	664	113	700	112	664	106	562	96	407	77	220	48	35	12	0	0
Aug	0	0	99	50	295	91	483	106	636	127	735	125	770	123	735	125	636	114	483	101	295	71	99	32	0	0
Sep	0	0	182	78	388	109	578	127	730	139	827	149	861	155	827	149	730	146	578	121	388	97	182	58	0	0
Oct	66	45	272	95	483	121	673	141	822	156	917	165	950	181	917	183	822	173	673	155	483	135	272	90	66	28
Nov	135	62	348	90	558	112	743	126	887	133	979	137	1010	131	979	137	887	142	743	134	558	117	348	87	135	45
Dec	157	58	375	83	587	103	773	108	917	119	1009	121	1040	114	1009	131	917	128	773	124	587	116	375	86	157	49